PHYSICAL REVIEW A VOLUME 27, NUMBER 2 FEBRUARY 1983

Theory of photoelectron angular distributions in resonant multiphoton ionization

S. N. Dixit
Corporate Research—Science Laboratories, Exxon Research and Engineering Company, P.O. Box 45, Linden, New Jersey 07036

P. Lambropoulos
Department of Physics, University of Southern California, Los Angeles, California 90007
(Received 5 August 1982)

In this paper, we present the theory of photoelectron angular distributions in resonant multiphoton ionization that rigorously takes into account the saturation, ac Stark-shift, and the laser-linewidth effects. The influence of these effects on the distribution is incorporated through the coupling equations between the angle-resolved ionization probabilities and the (time-dependent) bound-state density-matrix elements. General expressions for the angular distributions are derived and several properties of these distributions are arrived at from these expressions. Finally, numerical results are presented to illustrate the effects of saturation, of ac Stark shifts, and of the laser line shape.

I. INTRODUCTION

The study of photoelectron angular distributions is one of the basic tools for the exploration of atomic and molecular structure. In multiphoton ionization, however, such angular distributions acquire additional levels of complexity and variety.[1–7] As in single-photon ionization, the initial state plays a central role in determining the distribution. But two other aspects are equally important in a multiphoton transition: the order of the process and the possible participation of real intermediate states. The order of the process introduces features which are independent of the target atom; as, for example, the maximum order of the Legendre polynomial appearing in the distribution. One might say that it reflects the geometric features of the process. The participation of a real intermediate state on the other hand, reflects dynamical aspects of the process as well. Thus, in three-photon ionization, for example, the details of the distribution depend significantly on whether there is a single- or a two-photon resonance with an intermediate state. It is the effects associated with such resonant or near-resonant intermediate states that is the focus of our interest in this paper.

The photoelectron angular distribution under such resonance conditions can also be viewed as the distribution for ionization from an excited state: the resonant intermediate state. Thus, the problem is intimately related to the spectroscopy of excited states which is a topic of intense current interest.[2,5–7] Resonant multiphoton ionization, however, is known to require particular care in its interpretation because the resonant intermediate state can and does shift as well as broaden under the strong radiation required for the observation of the process. Moreover, the bandwidth and other stochastic properties of the laser radiation are known to affect the process in a profound way.[8] It might then seem that, in view of such complications, the prospects for a quantitative description of these processes are not very encouraging. Our intention here is to show that one can in fact develop a systematic theory which contains the important features of the process and allows for a quantitative comparison with experiment.

Our theme, therefore, is the photoelectron angular distribution in resonant multiphoton ionization and its dependence on the strength and bandwidth of the radiation.[9] It turns out, however, that this dependence is uninteresting if not trivial when we have only one intermediate state. It is the case of two closely spaced intermediate states—such as, for example, a fine-structure pair—that presents a number of surprises. First of all, the transitions from the initial to each of the two intermediate states may saturate at different rates as the intensity changes. Second, the two states may shift by different amounts with the possibility of their order becoming inverted with respect to the order in the bare atom. Third, the laser bandwidth may affect the angular distribution because it may affect the superposition of the channels via each of the states to the continuum. This would come about, for example, when the laser bandwidth is comparable to the energy separation of the two states and the laser line center does not coincide with the center of the distance between

the states. Needless to say, this relative position will in general change with light intensity as the states shift. The above three aspects are of course interrelated and the theoretical challenge lies in developing a model that includes all of them.

In the following sections, we have taken two-photon resonant three-photon ionization of Na as a case study and have developed a model that can be readily generalized to other cases. The calculations presented here are sufficiently detailed to allow comparison with experimental results when available.

II. THEORY

The discussion in this section will be divided into two subsections, the first dealing with the dynamics of the process and the second concerning the details of the observation and the effect of the dynamics on it. The former includes a description of the multiphoton absorption process in terms of either the amplitude, the density-matrix, or the resolvent operator equations. The effects of ac Stark shifts, saturation of the probabilities as well as the effects of the laser linewidth, are included here. The second subsection describes the observation process; i.e., measurement of the ionization probability, angular distribution, and/or spin polarization of the ejected photoelectrons. The influence of the dynamical effects are incorporated through appropriate coupling equations—differential equations involving the density-matrix elements between the bound states.

A. Dynamics of the absorption process

The process we have in mind is the ionization of an atom (initially in its ground state) by absorption of $n+1$ photons. As far as the evolution of the population in the bound states is concerned, the continuum can be eliminated in an adiabatic way. This is a well-known procedure and has been described elsewhere in the literature.[10,11] Such an elimination of the continuum gives rise to the shifts and widths to the bound states, the widths signifying the decay of the population to the continuum. The (reduced) bound-state dynamics can be simplified further if the frequency of an integral number of photons is in resonance with some intermediate state. In that case, the number of equations can be reduced to those connecting only the resonantly coupled states with the effects of the off-resonant bound states appearing in the form of Stark shifts of the resonant states and the effective matrix elements connecting them. Such a procedure has been widely employed in discussing resonant multiphoton processes.

Restricting ourselves then to the case of an n-photon resonant $(n+1)$-photon ionization of the ground ($S_{1/2}$) state of an alkali-metal atom, the resonantly coupled states are the $S_{1/2}$ ground state and the two (if other than an S state) fine-structure states near the n-photon resonance. The importance of treating both fine-structure resonant states in discussion of strong-field behavior of the process has been emphasized recently by us.[11,12] For the sake of simplicity we shall further restrict ourselves to two-photon resonant three-photon ionization of sodium via a $nD_{3/2,5/2}$ doublet. The generalization to the case of an arbitrary order process can easily be done with appropriate generalization of the atomic parameters.

Denoting by $|0\rangle$, $|1\rangle$, and $|2\rangle$ the states (in the $|lsjm_j\rangle$ representation) $|0\,\frac{1}{2}\,\frac{1}{2}\,\frac{1}{2}\rangle$ ($S_{1/2}$ ground state), $|2\,\frac{1}{2}\,\frac{3}{2}\,\frac{1}{2}\rangle$, and $|2\,\frac{1}{2}\,\frac{5}{2}\,\frac{1}{2}\rangle$ ($D_{3/2,5/2}$ near-resonant states), respectively, the density-matrix equations governing the time evolution of the three-state system coupled to the continuum can be written as[12]

$$
\begin{aligned}
\frac{d}{dt}\rho_{00} &= -\tfrac{1}{2}i(\Omega_{01}\rho_{10}-\text{c.c.}) - \tfrac{1}{2}i(\Omega_{02}\rho_{20}-\text{c.c.}) ,\\
\frac{d}{dt}\rho_{11} &= -\Gamma_1\rho_{11} + \tfrac{1}{2}i(\Omega_{01}\rho_{10}-\text{c.c.})\\
&\quad + \tfrac{1}{2}i(\Omega_{12}^{*}\rho_{12}-\text{c.c.}) ,\\
\frac{d}{dt}\rho_{22} &= -\Gamma_2\rho_{22} + \tfrac{1}{2}i(\Omega_{02}\rho_{20}-\text{c.c.})\\
&\quad - \tfrac{1}{2}i(\Omega_{12}\rho_{12}-\text{c.c.}) ,\\
&\left[\frac{d}{dt} - i\Delta_1 + \tfrac{1}{2}\Gamma_1 + 4b\,\frac{\beta^2}{\Delta_1^2+\beta^2}\right]\rho_{10}\\
&\quad = \tfrac{1}{2}i\Omega_{10}(\rho_{11}-\rho_{00}) - \tfrac{1}{2}i\Omega_{12}\rho_{20} + \tfrac{1}{2}i\Omega_{20}\rho_{12} ,\\
&\left[\frac{d}{dt} - i\Delta_2 + \tfrac{1}{2}\Gamma_2 + 4b\,\frac{\beta^2}{\Delta_2^2+\beta^2}\right]\rho_{20}\\
&\quad = \tfrac{1}{2}i\Omega_{20}(\rho_{22}-\rho_{00}) - \tfrac{1}{2}i\Omega_{21}\rho_{10} + \tfrac{1}{2}i\Omega_{10}\rho_{21} ,\\
&\left[\frac{d}{dt} + i(\omega_{12}+S_{12}) + \tfrac{1}{2}(\Gamma_1+\Gamma_2)\right]\rho_{12}\\
&\quad = -\tfrac{1}{2}i\Omega_{10}\rho_{02} + \tfrac{1}{2}i\Omega_{02}\rho_{10}\\
&\quad + \tfrac{1}{2}i(\Omega_{12}^{*}\rho_{11} - \Omega_{12}\rho_{22}) .
\end{aligned}
\tag{1}
$$

In the above equation, Ω_{01},Ω_{02} denote the two-photon Rabi frequencies for transitions from the ground state to states $|1\rangle$ and $|2\rangle$, respectively. Γ_1,Γ_2 denote the ionization widths of states 1 and 2, while $\Omega_{12}(=\Omega'_{12}-i\Omega''_{12})$ denotes the interference between the two ionization channels. Δ_1,Δ_2 are detunings of two photons from the (ac Stark-shifted) energy differences between the ground-state and the near-resonant states $|1\rangle$ and $|2\rangle$, respectively, and $\omega_{12}+S_{12}=\Delta_2-\Delta_1$. The details of these parameters can be found in Ref. 12. The effects of the laser line shape, which is assumed to arise from phase fluctuations, are included in the terms

$$4b\frac{\beta^2}{\Delta_k^2+\beta^2}\ ,\quad k=1,2\ .$$

In this phase diffusion model, the laser spectrum is Lorentzian near the center with the full width at half-maximum (FWHM) $2b$ and has a cutofff around $\beta\ (>b)$. The form of these terms is valid for β larger than other parameters in the process.[13]

Apart from the assumptions about the laser line shape and the adiabatic elimination of the off-resonant states and the continuum, the above equations are exact in describing the evolution of the three-level system with time. All the saturation effects are rigorously included in the solutions of the coupled differential equations (1).

B. Photoelectron angular distributions

Having described the "equations of motion" governing the dynamics of the bound-state system decaying into the continuum, let us analyze how this dynamics influences the properties of the ejected photoelectron. Experimentally measured quantities are the probability of ionization (IP) (which is proportional to the total ion signal), the angular distribution (AD) and/or the spin polarization (SP) of the ejected photoelectrons. Of these, the IP is given simply as the total loss of population from the bound-state system and can be written as

$$P(t)=1-\rho_{00}(t)-\rho_{11}(t)-\rho_{22}(t)\ . \tag{2}$$

In situations where the photoelectron angular distribution and its spin polarization are measured, calculating the total loss of population is not sufficient; one has to study the details of the population dynamics in the continuum. To do this, we employ the partial-wave expansion of the continuum wave function as [14,15]

$$|f_{\vec{k}},\mu_f\rangle=4\pi\left[\frac{\pi}{2k}\right]^{1/2}\sum_{l=0}^{\infty}\sum_{m=-l}^{l}(i)^l e^{-i\delta_l}\times Y^*_{lm}(\hat{k})Y_{lm}(\hat{r})\times R_{El}(r)\chi_{\mu_f}\ , \tag{3}$$

where the radial functions $R_{El}(r)$ are assumed normalized on the energy scale,

$$\int_0^\infty R_{El}R_{E'l}r^2dr=\delta(E-E')=\delta(\tfrac{1}{2}k^2-\tfrac{1}{2}(k')^2) \tag{4}$$

and have the asymptotic form given by[16]

$$R_{El}(r)\underset{r\to\infty}{\to}\left[\frac{2}{\pi k}\right]^{1/2}\frac{1}{r}\sin(kr-l\pi/2-\delta_l)\ . \tag{5}$$

In Eq. (3), χ_{μ_f} denotes the spin-wave function of the electron with μ_f as the projection of its spin along the quantization axis ($\mu_f=\pm\frac{1}{2}$) and $Y_{lm}(\hat{r})$ and $Y_{lm}(\hat{k})$ denote the spherical harmonics for the orientation of the photoelectron position and its momentum, respectively.

For atoms exhibiting strong spin-orbit coupling, the radial function depends on the total angular momentum j, and the partial-wave expansion (3) has to be generalized as

$$|f_{\vec{k}},\mu_f\rangle=4\pi\left[\frac{\pi}{2k}\right]^{1/2}\sum_{l=0}^{\infty}\sum_{m=-l}^{l}(i)^l e^{-i\delta_l}Y^*_{lm}(\hat{k})\sum_{j,m_j}(-1)^{1/2-l-m_j}(2j+1)^{1/2}R_{Elj}(r)\times\begin{pmatrix} l & \frac{1}{2} & j\\ m & \mu_f & -m_j\end{pmatrix}|l\,\tfrac{1}{2}\,jm_j\rangle\ ; \tag{6}$$

note that $|f_{\vec{k}},\mu_f\rangle$ is normalized so that

$$\rho(k)\int\langle f_{\vec{k}},\mu_f|f_{\vec{k}},\mu_f\rangle d^3k=1,$$

where

$$\rho(k)=\frac{1}{(2\pi)^3} . \tag{7}$$

The phase shift δ_l of the l partial wave is the sum of the Coulomb phase shift $\arg(\Gamma(l+1-i/k))$ and the shift due to the quantum defect $\pi\mu_l$, where μ_l is the extrapolated quantum defect for the l states.

The probability that an electron will be ejected at an angle (θ,ϕ) with respect to the z axis and will have $\mu_f=\pm\frac{1}{2}$, denoted by $P_{\pm}(\theta,\phi)$, obeys the differential equation

$$\frac{dP_{\pm}(\theta,\phi)}{dt}=\Gamma_1^{\pm}(\theta,\phi)\rho_{11}+\Gamma_2^{\pm}(\theta,\phi)\rho_{22}+\Omega_{12}''^{\pm}(\theta,\phi)2\,\mathrm{Re}\rho_{12} \tag{8}$$

whose derivation is sketched in the Appendix. The direction-dependent width parameters $\Gamma_1^{\pm}(\theta,\phi)$, $\Gamma_2^{\pm}(\theta,\phi)$, and $\Omega_{12}''^{\pm}(\theta,\phi)$ are defined as

$$\begin{aligned}
\Gamma_1^{\pm}(\theta,\phi)&=2\pi\alpha F\omega\frac{k}{(2\pi)^2}\langle 1\,|\,\vec{r}\cdot\vec{\epsilon}^{\,*}\,|\,f_{\vec{k}},\mu_f\rangle\langle f_{\vec{k}},\mu_f\,|\,\vec{r}\cdot\vec{\epsilon}\,|\,1\rangle ,\\
\Gamma_2^{\pm}(\theta,\phi)&=2\pi\alpha F\omega\frac{k}{(2\pi)^2}\langle 2\,|\,\vec{r}\cdot\vec{\epsilon}^{\,*}\,|\,f_{\vec{k}},\mu_f\rangle\langle f_{\vec{k}},\mu_f\,|\,\vec{r}\cdot\vec{\epsilon}\,|\,2\rangle ,\\
\Omega_{12}''^{\pm}(\theta,\phi)&=2\pi\alpha F\omega\frac{k}{(2\pi)^2}\langle 2\,|\,\vec{r}\cdot\vec{\epsilon}^{\,*}\,|\,f_{\vec{k}},\mu_f\rangle\langle f_{\vec{k}},\mu_f\,|\,\vec{r}\cdot\vec{\epsilon}\,|\,1\rangle
\end{aligned} \tag{9}$$

with $\pm$ corresponding to $\mu_f=\pm\frac{1}{2}$, and are related to the total widths Γ_1, Γ_2, and Ω_{12}'' used in Eq. (1) by

$$\begin{aligned}
\Gamma_1&=\int d\Omega_k(\Gamma_1^{+}(\theta,\phi)+\Gamma_1^{-}(\theta,\phi)) ,\\
\Gamma_2&=\int d\Omega_k(\Gamma_2^{+}(\theta,\phi)+\Gamma_2^{-}(\theta,\phi)) ,
\end{aligned}$$

and

$$\Omega_{12}''=\int d\Omega_k(\Omega_{12}''^{+}(\theta,\phi)+\Omega_{12}''^{-}(\theta,\phi)) . \tag{10}$$

The above expressions for the widths can be simplified further by using the partial-wave expansion of the continuum wave function given in Eq. (6).

Consider the matrix element

$$A_{nljm_j}^{k\mu_f\chi q}=\left\langle f_{\vec{k}},\mu_f\left|r^{\chi}\left[\frac{4\pi}{2\chi+1}\right]^{1/2}Y_{\chi q}\right|R_{nlj}\,l\,\tfrac{1}{2}\,jm_j\right\rangle \tag{11}$$

representing the 2χ-pole transition between the state $|\,R_{nlj}\,l\,\frac{1}{2}\,jm_j\rangle$ and the continuum ($\chi=1,q=0$ for electric dipole transitions with light linearly polarized along the z direction while $\chi=2,q=\pm1$ for electric quadrupole transitions in the presence of light linearly polarized along the z direction). Using the continuum-state expansion given in (6) and the well-known theorems on angular-momentum algebra,[14,17] $A_{nljm_j}^{k\mu_f\chi q}$ can be written as

$$A_{nljm_j}^{k\mu_f\chi q}=4\pi\left[\frac{\pi}{2k}\right]^{1/2}\sum_{l_1=0}^{\infty}\sum_{m_{l_1}=-l_1}^{l_1}(-i)^{l_1}e^{i\delta_{l_1}}\sum_{j_1,m_{j_1}}R_{nlj;El_1j_1}^{\chi}Y_{l_1m_{l_1}}(\hat{k})C_{ljm_j;l_1j_1m_{l_1}\mu_fm_{j_1}}^{\chi q} , \tag{12}$$

where the purely algebraic coefficients $C_{ljm_j;l_1j_1m_{l_1}\mu_fm_{j_1}}^{\chi q}$ (chosen to be real) are defined in terms of the 3-j and 6-j symbols[14,17] as

$$\begin{aligned}
C_{ljm_j;l_1j_1m_{l_1}\mu_fm_{j_1}}^{\chi q}&=(-1)^{l_1+j_1+j+\chi+1-2m_{j_1}}(2j_1+1)[(2l_1+1)(2l+1)(2j+1)]^{1/2}\begin{pmatrix}l_1 & \frac{1}{2} & j_1\\ m_{l_1} & \mu_f & -m_{j_1}\end{pmatrix}\\
&\times\begin{pmatrix}j_1 & \chi & j\\ -m_{j_1} & q & m_j\end{pmatrix}\begin{pmatrix}l_1 & \chi & l\\ 0 & 0 & 0\end{pmatrix}\begin{Bmatrix}l_1 & j_1 & \frac{1}{2}\\ j & l & \chi\end{Bmatrix}
\end{aligned} \tag{13}$$

and

$$R^{\chi}_{nlj;El_1j_1} = \int_0^{\infty} R_{El_1j_1} r^{\chi} R_{nlj} r^2 dr \ . \tag{14}$$

A product of two bound-free matrix elements such as those appearing in Eq. (9) can then be expressed as

$$B^{k\mu_f\chi q}_{nljm_j;n'l'j'm'_j} = A^{k\mu_f\chi q*}_{nljm_j} A^{k\mu_f\chi q}_{n'l'j'm'_j}$$

$$= \frac{8\pi^3}{k} \sum_{\substack{l_1,l_2,j_1,j_2,\\ m_{l_1},m_{l_2}\\ m_{j_1},m_{j_2}}} (-i)^{l_1-l_2} e^{i(\delta_{l_1}-\delta_{l_2})} R^{\chi}_{nlj;El_1j_1} R^{\chi}_{n'l'j';El_2j_2}$$

$$\times C^{\chi q}_{l'j'm'_j;l_2j_2m_{l_2}\mu_f m_{j_2}} C^{\chi q}_{ljm_j;l_1j_1m_{l_1}\mu_f m_{j_1}} Y_{l_1m_{l_1}}(k) Y^*_{l_2m_{l_2}}(k) \ . \tag{15}$$

Finally, with the help of the identity (Ref. 17, Eq. 1.43)

$$Y^*_{l_2m_2} Y_{l_1m_1} = (-1)^{m_2} \sum_{L,M} \left[\frac{(2l_1+1)(2l_2+1)(2L+1)}{4\pi} \right]^{1/2} Y^*_{LM} \begin{pmatrix} l_1 & l_2 & L \\ 0 & 0 & 0 \end{pmatrix} \begin{pmatrix} l_1 & l_2 & L \\ m_1 & -m_2 & M \end{pmatrix}, \tag{16}$$

Eq. (15) can be rewritten as

$$B^{k\mu_f\chi q}_{nljm_j;n'l'j'm_{j'}} = \frac{8\pi^3}{k} \sum_{\substack{l_1,l_2,j_1,j_2,\\ m_{l_1},m_{l_2},m_{j_1},m_{j_2}}} (-i)^{l_1-l_2} e^{i(\delta_{l_1}-\delta_{l_2})} R^{\chi}_{nlj;El_1j_1} R^{\chi}_{n'l'j';El_2j_2} C^{\chi q}_{ljm_j;l_1j_1m_{l_1}\mu_f m_{j_1}} C^{\chi q}_{l'j'm_{j'};l_2j_2m_{l_2}\mu_f m_{j_2}}$$

$$\times (-1)^{m_{l_2}} \sum_{L,M} \left[\frac{(2l_1+1)(2l_2+1)(2L+1)}{4\pi} \right]^{1/2}$$

$$\times Y^*_{LM}(\theta,\Phi) \begin{pmatrix} l_1 & l_2 & L \\ 0 & 0 & 0 \end{pmatrix} \begin{pmatrix} l_1 & l_2 & L \\ m_{l_1} & -m_{l_2} & M \end{pmatrix}. \tag{17}$$

This is the main expression of our paper. All the details of the angular distribution and the spin polarization are contained in the coefficients appearing in this equation.

Several general statements about the angular distributions can be made at this point without explicitly calculating any of the coefficients. These conclusions follow from the properties of the 3-j symbols. In arriving at these conclusions it is assumed that only one type of multipole interaction is present (only one set of χ,q allowed). Effects of more than one multipole interaction on the distribution are discussed a little later.

Because the 3-j symbol

$$\begin{pmatrix} j_1 & j_2 & j_3 \\ 0 & 0 & 0 \end{pmatrix}$$

vanishes unless the sum $j_1 + j_2 + j_3$ is even,[17] it follows that only those values of L's appear in Eq. (17) that satisfy the condition

$$l + l' + L = \text{even} \ . \tag{18}$$

If the states $| l \tfrac{1}{2} j m_j \rangle$ and $| l' \tfrac{1}{2} j' m_{j'} \rangle$ were reached by absorbing the same number of photons from some common state, then $l - l'$ is even which implies that L is even. Thus only even order Y_{LM}'s remain in Eq. (17).

If $m_j = m'_j$ and $l - l'$ is even, as would be the case if the same number of photons were absorbed from some given state to reach the states $| R_{nlj}\, l \tfrac{1}{2} j m_j \rangle$ and $| R_{n'l'j'} l' \tfrac{1}{2} j' m'_j \rangle$, it follows that $m_1 = m_2$ and hence $M = 0$ along with the fact that L is even. Hence, only even-order Legendre polynomials appear in the expression for the angular distributions. Such an expansion of the angular distribution in terms of even-order Legendre polynomials has been

widely employed in the discussions on multiphoton angular distributions.[1,18]

Note that the interference terms between different partial waves ($l_1 \neq l_2$) disappear in the integrated cross section because of the relation

$$\begin{pmatrix} l_1 & l_2 & 0 \\ m_1 & -m_2 & 0 \end{pmatrix} = (-1)^{-l_2+m_2} \frac{\delta_{l_1 l_2}\delta_{m_1 m_2}}{\sqrt{2l_1+1}} . \quad (19)$$

A comment is in order at this point. All of the above expressions have been derived assuming that a single multipole of the radiation field is important in the ionization process. If the dipole approximation is valid, this will indeed be the case. Whenever higher multipoles contribute to the ionization process, the factor $r^{\chi}Y_{\chi q}$ in (9) has to be generalized to a sum of the important multipoles and the angular-momentum algebra carried out in an appropriate manner. Then in addition to the partial-wave interferences, one also gets interferences between various multipoles.

For the remainder of this section we shall restrict ourselves to n-photon resonant $(n+1)$ photon ionization of the $S_{1/2}$ ground state of an alkali-metal atom by light linearly polarized in the z direction ($\chi=1$, $q=0$). In this case, the maximum allowed values of l,l' is n and that of l_1,l_2 is $(n+1)$. Furthermore, $m_j=m_j'$ which implies $M=0$ and there is no ϕ dependence of the angular distribution. Clearly only even-order Legendre polynomials from $L=0$ up to $L=2(n+1)$ appear in Eq. (17). $B^{k\mu_f 10}_{nljm_j;n'l'j'm_j}$ can then be expanded as

$$B^{l(\mu_f=\pm\frac{1}{2})10}_{nljm_j;n'l'j'm_j'} = \sum_{p=0}^{n+1} A^{\pm}_{nljm_j;n'l'j'm_j';2p} P_{2p}(\cos\theta) , \quad (20)$$

where

$$A^{\pm}_{nljm_j;n'l'j'm_j';2p} = \frac{2\pi^2}{k}(4p+1) \sum_{\substack{l_1,l_2,\\ m_{l_1},j_1,j_2}} (-i)^{l_1-l_2} e^{i(\delta_{l_1}-\delta_{l_2})} R^{\chi}_{nlj;El_1j_1} R^{\chi}_{n'l'j';El_2j_2}$$

$$\times C^{\chi q}_{l'j'm_j',l_1j_1m_{l_1}\mu_f m_{j_1}} C^{\chi q}_{ljm_j,l_2j_2m_{l_1}\mu_f m_{j_2}} (-1)^{m_{l_1}} \begin{pmatrix} l_1 & l_2 & 2p \\ 0 & 0 & 0 \end{pmatrix} \begin{pmatrix} l_1 & l_2 & 2p \\ m_{l_1} & -m_{l_1} & 0 \end{pmatrix} . \quad (21)$$

With the help of Eqs. (9) and (10), $\Gamma_1^{\pm}(\theta,\phi)$, $\Gamma_2^{\pm}(\theta,\phi)$, and $\Omega_{12}''^{\pm}(\theta,\phi)$ can also be expanded in terms of $P_{2p}(\cos\theta)$ as

$$\begin{aligned} \Gamma_1^{\pm}(\theta) &= \sum_{p=0}^{n+1} b^{\pm}_{11(2p)} P_{2p}(\cos\theta) , \\ \Gamma_2^{\pm}(\theta) &= \sum_{p=0}^{n+1} b^{\pm}_{22(2p)} P_{2p}(\cos\theta) , \\ \Omega_{12}''^{\pm} &= \sum_{p=0}^{n+1} b^{\pm}_{12(2p)} P_{2p}(\cos\theta) . \end{aligned} \quad (22)$$

$b^{\pm}_{ij(2p)}$ are simply products of the factor $A^{\pm}_{nljm_j;n'l'j'm_j';2p}$ in Eq. (21) with proper $nljm_j$ as defined in Sec. II A and the factor $[k/(2\pi)^2]2\pi\alpha F\omega$ from Eq. (9).

Another important property that follows quite generally is that if $j=l-\frac{1}{2}$ for a given l state ($D_{3/2}$ state, for example), then

$$A^{+}_{nljm_j;n'ljm_j;2(l+1)} = -A^{-}_{nljm_j;nljm_j;(2l+2)} .$$

This implies that the width summed over the photoelectron spin for this state does not contain the Lengendre polynomial of the highest order $(2l+2)$. Specifically, since $|1\rangle = |2\,\frac{1}{2}\,\frac{3}{2}\,\frac{1}{2}\rangle$, $\Gamma_1(\theta)=\Gamma_1^{+}(\theta) + \Gamma_1^{-}(\theta)$ contains terms only up to $P_4(\cos\theta)$.

One can alternatively expand $\Gamma_1^{\pm}(\theta)$, etc., in terms of even powers of $\cos\theta$ simply by expanding the $P_{2p}(\cos\theta)$. Thus,

$$\begin{aligned} \Gamma_1^{\pm}(\theta) &= \sum_{k=0}^{n+1} a^{\pm}_{11(2k)} \cos^{2k}\theta , \\ \Gamma_2^{\pm}(\theta) &= \sum_{k=0}^{n+1} a^{\pm}_{22(2k)} \cos^{2k}\theta , \\ \Omega_{12}''^{\pm}(\theta) &= \sum_{k=0}^{n+1} a^{\pm}_{12(2k)} \cos^{2k}\theta , \end{aligned} \quad (23)$$

where

$$a^{\pm}_{ij(2k)} = \sum_{p=0}^{n+1} b^{\pm}_{ij(2p)} C^{2k}_{2p}$$

and

$$P_{2p}(\cos\theta) = \sum_{k=0}^{p} C^{2k}_{2p} \cos^{2k}(\theta) , \quad (24)$$

C_{2p}^{2k} being the expansion coefficients for the Legendre polynomials.

Expanding $P_{\pm}(\theta)$ in terms of $\cos^{2k}\theta$ as

$$P_{\pm}(\theta)=\sum_{k=0}^{n+1} P_{2k}^{\pm}\cos^{2k}(\theta) , \tag{25}$$

the coefficients $P_{2k}^{\pm}$ obey

$$\frac{dP_{2k}^{\pm}}{dt}=a_{11(2k)}^{\pm}\rho_{11}+a_{22(2k)}^{\pm}\rho_{22}+2a_{12(2k)}^{\pm}\mathrm{Re}\rho_{12} . \tag{26}$$

This is the connecting equation describing the influence of the bound-state dynamics on the angular distribution and the spin polarization of the photoelectron. Saturation effects appear through the time-dependent density-matrix elements ρ_{11}, ρ_{22}, and ρ_{12} whose behavior is governed by Eq. (1). If one is interested in studying only the spin polarization of the photoelectron, as was done in Ref. 12, $P_{\pm}(\theta)$ has to be integrated over the angles

$$P_{\pm}=2\pi\int_0^{\infty} P_{\pm}(\theta)\sin\theta\, d\theta=4\pi\sum_{k=0}^{n+1}\frac{P_{2k}^{\pm}}{(2k+1)} , \tag{27a}$$

while investigating the angular distributions alone requires that we sum the IP over the spin of the ejected electron,

$$P(\theta)=P_{+}(\theta)+P_{-}(\theta),\quad P_{2k}=P_{2k}^{+}+P_{2k}^{-} . \tag{27b}$$

For a complete measurement of all the atomic parameters as done in recent experiments,[6] one must study $P_{\pm}(\theta)$ itself.

For weak fields, lowest-order solutions for ρ_{11}, ρ_{22}, and ρ_{12} can be obtained from (1), which, after substitution in (26) yield the familiar Fermi golden rule for the ionization probability per unit time.[19]

An observation that can be made easily from the expansion of $P(\theta,\phi)$ in terms of $\cos^{2k}\theta$ is that for an odd-photon ionization of an S state in the absence of spin-orbit coupling (SOC), all the $a_{ij0}^{+}+a_{ij0}^{-}=0$; i.e., there is no constant term in the angular distribution: $P_0=0$. This is so because $m_1=m_2=0$ in the absence of SOC and l_1,l_2 are both odd because of odd-photon ionization of an S state. Thus, only $Y_{l_1 0}, Y_{l_2 0}$ with odd l_1, l_2 appear in Eq. (15) which have no constant terms implying that $a_{ij0}^{+}+a_{ij0}^{-}=0$.

In off-resonant multiphoton ionization of ground-state alkali-metal atoms, the SOC can be neglected and this yields $P_0=0$. Note further that P_0 is amenable to direct observation as $P(\theta=\pi/2)=P_0$. One would measure P_0 by measuring the ion signal in the direction perpendicular to the direction of the light polarization.

Strong-field effects due to the ac Stark shifts as well as due to the saturation of the IP influence the behavior of the angular distribution through their influence on the density-matrix elements ρ_{11}, ρ_{22}, and ρ_{12} in Eq. (26). In discussing these effects, it is convenient to normalize the distribution in a suitable manner. In this paper, we shall normalize the AD so that the integrated area under the distribution is unity. The normalized coefficients P_{2k} are defined as

$$p_{2k}^{\pm}=P_{2k}^{\pm}/P , \tag{28}$$

where

$$P=\int d\Omega_k[P_{+}(\theta)+P_{-}(\theta)]$$

is the total ionization probability. Furthermore, we shall sum over the photoelectron spin as our emphasis here is on its angular distribution. Saturation effects on the photoelectron spin polarization have been discussed in detail elsewhere.[12] Thus, we concentrate here on the behavior of the coefficients

$$p_{2k}=p_{2k}^{+}+p_{2k}^{-}=(P_{2k}+P_{2k})/P . \tag{29}$$

Formal integration of (26) yields

$$P_{2k}=P_{2k}^{+}+P_{2k}^{-}=\int_0^t a_{11k}\rho_{11}dt+\int_0^t a_{22k}\rho_{22}dt+\int_0^t a_{12k}2\,\mathrm{Re}\rho_{12}dt , \tag{30}$$

while

$$P=\int_0^t \Gamma_1\rho_{11}dt+\int_0^t \Gamma_2\rho_{22}dt+\int_0^t \Omega_{12}''2\,\mathrm{Re}\rho_{12}dt .$$

It is worth noting that any change in the normalized distribution due to saturation occurs because of the differential saturation of the two ionization channels. For, if the ionization were to take place via only one intermediate resonant state, for example, $|1\rangle$, then $\int_0^t\rho_{11}dt$ would disappear from the definition of the normalized coefficients p_{2k} and $p_{2k}=a_{11(2k)}/\Gamma_1$ irrespective of saturating conditions.

For very long interaction times, all the population has already decayed to the continuum and thus ρ_{11}, ρ_{22}, and ρ_{12} are vanishingly small. Therefore, the area under these density-matrix elements does not change with further increases in time. Hence, P_{2k} reach their asymptotic values and furthermore, this limiting distribution is not isotropic. For a uniform excitation field ($a_{ij(2k)}=$const), areas under ρ_{11}, ρ_{22}, and ρ_{12} can be obtained by Laplace transforming Eq. (1) and evaluating $\hat{\rho}_{11}(s=0)$, $\hat{\rho}_{22}(s=0)$, $\hat{\rho}_{12}(s=0)$ [$\hat{\rho}_{ij}(s)$ denotes the Laplace transform of $\rho_{ij}(t)$]. Although analytic expressions can be obtained by inverting the coefficient matrix of Eq. (1), the results

are not sufficiently transparent to warrant this publication. The limiting behavior is, however, discussed on the basis of numerical results in Sec. III.

For two-photon resonant three-photon ionization, the angular distribution can be written as

$$P(\theta)=P_0+P_2\cos^2\theta+P_4\cos^4\theta+P_6\cos^6\theta \ .$$

This distribution is symmetric about $\theta=0$, $\pi/2$, π, and $3\pi/2$ and one need only look at one quadrant (for example, $0\leq\theta\leq\pi/2$). To emphasize the shape, we shall plot $P(\theta)$ for $0\leq\theta\leq2\pi$ with the understanding that $P(\theta)$ for $\pi\leq\theta\leq2\pi$ corresponds to $P(\theta,\phi=3\pi/2)$ $[=P(\theta,\phi=\pi/2)$ as there is no ϕ dependence] with $0\leq\theta\leq\pi$. Along with the extrema at $\theta=0$, $\pi/2$, π, and $3\pi/2$, $P(\theta)$ will have extrema at angles satisfying

$$3P_6\cos^4\theta+2P_4\cos^2\theta+P_2=0 \ . \tag{31}$$

We shall characterize a distribution as being two lobed, one lobed, or as having no lobes according to whether the above equation has two, one, or zero solutions for the angle θ. How many lobes will appear in the distribution depends on the number of solutions of (31) that satisfy $0\leq\cos^2\theta\leq1$. This imposes restrictions on the parameters P_2, P_4, and P_6.

Finally, we conclude this section with a remark about the multiphoton angular distributions in general. From Eq. (15), it is clear that all the information about the angular distributions is contained in the expressions $B^{k\mu_f\chi q}_{nljm_j;n'l'j'm_j'}$. The differential cross section for photoionization of a given $|nljm_j\rangle$ state is proportional to

$$\sum_{\mu_f} B^{k\mu_f\chi q}_{nljm_j;nljm_j} \ .$$

This expression still has to be averaged over the initial-state magnetic quantum number m_j. Let $w(m_j)$ denote the occupation probabilities for the state $|nljm_j\rangle$. Then we can define an averaged differential cross section as

$$\frac{d\sigma}{d\Omega_k}=\sum_{m_j} w(m_j)\sum_{\mu_f} B^{k\mu_f\chi q}_{nljm_j;nljm_j} \ . \tag{32}$$

In the above equation, all the irrelevant constants have been suppressed for the sake of clarity. If the initial state is unpolarized as would be the case in single photoionization of a ground state, the occupation probabilities $w(m_j)$ are all equal to $1/(2j+1)$; Eq. (32) then simplifies to

$$\frac{d\sigma}{d\Omega_k}=\frac{1}{(2j+1)}\sum_{m_j,\mu_f} B^{k\mu_f\chi q}_{nljm_j;nljm_j} \ . \tag{33}$$

After straightforward but tedious algebra, the summations can be performed analytically and the above equation can be rewritten as

$$\frac{d\sigma}{d\Omega_k}=\text{const}\sum_L(-1)^q\frac{\hat{L}}{4\pi}P_L(\cos\theta)\begin{pmatrix}\chi & \chi & L\\ -q & q & 0\end{pmatrix}g_L \ , \tag{34}$$

where

$$g_L=\sum_{\substack{l_1,l_2\\ j_1,j_2,\\ j_t}}(-i)^{l_1-l_2}e^{i(\delta_{l_1}-\delta_{l_2})}R^{\chi}_{nlj;El_1j_1}R^{\chi}_{nlj;El_2j_2}(-1)^{l_1+l_2+j_t}\hat{l}\hat{l}_1\hat{l}_2\hat{j}_1\hat{j}_2\hat{j}_t\begin{pmatrix}l_1 & \chi & l\\ 0 & 0 & 0\end{pmatrix}\begin{pmatrix}l_2 & \chi & l\\ 0 & 0 & 0\end{pmatrix}\begin{pmatrix}l_1 & l_2 & L\\ 0 & 0 & 0\end{pmatrix}$$

$$\times\begin{Bmatrix}\chi & \chi & L\\ l_1 & l_2 & j_t\end{Bmatrix}\begin{Bmatrix}j & \chi & j_1\\ l_1 & \frac{1}{2} & j_t\end{Bmatrix}\begin{Bmatrix}l_1 & j_1 & \frac{1}{2}\\ j & l & \chi\end{Bmatrix}\begin{Bmatrix}l_2 & j_2 & \frac{1}{2}\\ j & l & \chi\end{Bmatrix}\begin{Bmatrix}j & \chi & j_2\\ l_2 & \frac{1}{2} & j_t\end{Bmatrix} \ , \tag{35}$$

where

$$\hat{l}=(2l+1) \ ,$$

etc. Equation (34) reveals an interesting feature that in single photoionization of an unpolarized state, the photoelectron angular distribution contains even-order Legendre polynomials of order 0 to 2χ ($\chi=1$ for a dipole transition, $\chi=2$ for quadrupole, etc.). This is just a restatement of the well-known theorem by Yang.[30] For photoionization by a dipole photon ($\chi=1$), the angular distribution (34) is of the form $a+bP_2(\cos\theta)$, a form that is widely used in the discussion of effects of atomic structure on the photoelectron angular distribution.

The multiphoton angular distributions, on the other hand, can be viewed as angular distributions arising from the photoionization of a polarized ini-

tial state [$w(m_j)$ not same for all m_j]. The signature of the multiphoton character of the process is passed through the creation of an uneven distribution in the states $|nljm_j\rangle$. The weights $w(m_j)$, being proportional to the square of the Rabi frequency for the transition from the ground state to the resonant state $|nljm_j\rangle$, reflect the characteristics of the multiphoton nature of the absorption process through the specific m_j dependence of the Rabi frequencies. Angular distributions from ionization of an excited state prepared by other means would be different from the multiphoton ionization angular distributions due to different relationships between the weights $w(m_j)$.

III. NUMERICAL CALCULATIONS AND DISCUSSION

In this section we shall illustrate some of the effects described in Sec. II with the help of numerical calculations of the angular distributions. These calculations have been performed for two-photon resonant three-photon ionization of the $3S_{1/2}$ ground state of sodium via the inverted $4D_{5/2,3/2}$ doublet separated by 0.0346 cm^{-1} ($=\omega_{12}$). For interaction times of a few ns, the precession of the density-matrix elements due to the hyperfine splitting (hf) is small (precession period $\sim 1/\Delta_{hf}$) and the description of the ionization process in terms of the fine-structure scheme is adequate. For long interaction times and/or large hyperfine splittings, the problem has to be analyzed in the hyperfine scheme as has been done for the two-photon ionization process.[21] This treatment, however, is not complete since rate equations have been used in Ref. 21 to describe the two-photon ionization process. The atomic parameters were calculated using the quantum-defect theory and are given below (see Ref. 12 for a description of these parameters). All the parameters are in rad/sec and I denotes the laser intensity in W/cm^2:

$$\Omega_{10}=-556.0I,\quad \Omega_{20}=713.3I,\quad \Gamma_1=9.361I,$$
$$\Gamma_2=9.584I,$$
$$S_0=1310I,\quad S_1=175.2I,\quad S_2=190.7I,$$
$$\Omega'_{12}=-39.52I,\quad \Omega''_{12}=-0.546I.$$

Angular distribution parameters for this process are

$$a_{110}=0.556I,\quad a_{112}=-1.111I,$$
$$a_{114}=2.798I,\quad a_{116}=0,$$
$$a_{220}=0.3705I,\quad a_{222}=3.434I,$$
$$a_{224}=-12.09I,\quad a_{226}=11.64I,$$
$$a_{120}=0.454I,\quad a_{122}=-11.15I,$$
$$a_{124}=36.46I,\quad a_{126}=-28.51I.$$

It is known that turning the field on instantaneously (as is implied in a square-pulse approximation) gives rise to unphysical populations of the excited states.[22] To eliminate such populating of the states we assume that the intensity rises linearly for zero to its maximum value in a time τ and remains constant thereafter. Equations (1) and (26) are integrated numerically up to time τ and the Laplace-transform method is used for $t>\tau$ with the values of ρ_{ij} at τ as initial conditions. We have found that $\tau=0.1$ nsec is sufficient to remove the transients and τ has, therefore, been set to this value for all the results presented in this paper.

Note that there are two types of interference in the process. First, there is the interference between the P and the F partial waves in the continuum which is proportional to the product of the $D\rightarrow P$ and $D\rightarrow F$ bound-free radial matrix elements R_1 and R_3, respectively, and to the cosine of the difference in the phase shifts $(\delta_1-\delta_3)$ for the P and F waves. For photon energies near the $4D$ resonances, we find $R_1 \ll R_3$. Thus, the $P-F$ interference contribution, as well as the P partial-wave contribution to the coefficients $a_{ij(2k)}$ are small. The second type of interference occurs betwen the ionization channels that proceed via states $|1\rangle$ and $|2\rangle$. This is characterized by Ω''_{12} and $a_{12(2k)}$ terms and is a dynamical effect because of its dependence on ρ_{12} in Eq. (26). Note that although Ω''_{12} is small compared to Γ_1,Γ_2, $a_{12(2k)}$ are comparable to or larger than $a_{jj(2k)}$. This implies that the angular distribution will be quite sensitive to this dynamical interference. This is illustrated below.

In Fig. 1 we have plotted a series of angular distributions for various values of the laser intensity. The photon frequency is tuned to the $D_{5/2}$ resonance in the absence of Stark shifts. For low powers (0.5 MW) the $D_{3/2}$ level, being detuned from resonance, influences the distribution very little and the resulting distribution resembles the one obtained assuming only the $D_{5/2}$ state present. With increasing intensity, the ac Stark shifts become large and move the levels in and out of resonance. This is reflected through the changes in the angular distributions. Note that the magnitudes of the relative shifts (with the ground state) are such that the dynamic separation between the ground and excited states decreases with increasing intensity. Furthermore, S_{12} is negative and at some intensity will cancel out ω_{12}. Thus, there will be a field-induced crossing of the $4D$ doublet at this value of the laser power. At 1 MW/cm^2, the lobes disappear due to the interfer-

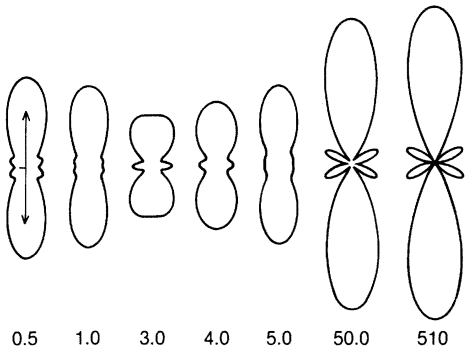

FIG. 1. Photoelectron angular distributions for a two-photon resonant three-photon ionization of sodium. The laser intensities (in MW/cm^2) are shown under each plot. Other parameters are laser duration $t=5$ nsec, its bandwidth $b=0$, and its frequency ω is such that $2\omega=\omega_{4D_{5/2}}-\omega_{3S_{1/2}}$. The arrow indicates the direction of light polarization with respect to which θ is measured. The radial scale is the same for all the plots.

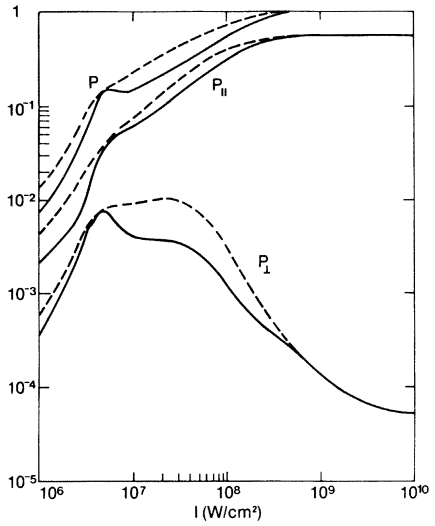

FIG. 2. Multiphoton ionization probability as a function of the laser power. P, $P_{||}$, and $P_{\perp}$ correspond, respectively, to the total ionization probability, and the ionization probabilities in a direction parallel and perpendicular to the direction of light polarization. Solid curves correspond to a monochromatic field and the dashed lines to a field having full width at half maximum 0.002 cm^{-1}.

ence of the two ionization channels while for higher intensities the distribution reemerges as a one-lobed structure when the dynamic detuning of the $D_{3/2}$ state is small. With further increases in intensity, both levels move away from resonance while the IP begins to saturate. This causes the distribution to reach an asymptotic shape where the lobes are very sharp. We find that this shape is quite different from the one predicted by the lowest-order perturbation theory and is insensitive to further increases in intensity, interaction time, and detuning; the insensitivity occurs due to the indistinguishability of the two fine-structure states that were near resonant at low intensities but have been shifted far away from resonance at high intensities.

In Fig. 2 we have plotted the ionization probabilities for ejecting an electron along the direction of light polarization $[P_{||}=P(\theta=0)]$ and perpendicular to it $[P_{\perp}=P(\theta=\pi/2)]$ along with the total ionization probability (P). The most important effect observed in this graph is the decrease of $P_{\perp}$ at large intensities. Note that with increasing intensity the D levels are shifted farther and farther away from resonance and hence become indistinguishable and the ionization process proceeds as if the spin-orbit coupling were small. Under such circumstances, it follows, from the arguments presented in Sec. II, that P_0 would vanish since the minimum number of photons required for ionization is odd. $P_{||}$ and P do not exhibit any such decrease since P_2, P_4, P_6 are nonzero even in the absence of spin-orbit coupling. Other features of this graph have already been discussed in our earlier paper.[9]

Let us discuss the limiting behavior of the angular distribution a little further. From Eq. (30) it is obvious that it depends on the area under the curves of ρ_{11}, ρ_{22}, and $\mathrm{Re}\rho_{12}$ as a function of time, hence, on the details of the dynamics for all times. Being close to or far away from resonance with $|1\rangle$ or $|2\rangle$ alters the evolution of the density-matrix elements and hence the area under them. An asymptotically constant value for the limiting distribution is reached only when the area under the curves changes little with changes in external parameters. In Fig. 1 this occurs at about the same power at which the ionization probability saturates. The fact that this need not be so is illustrated in Fig. 3 where we have again plotted a series of distributions for different laser intensities. All the atomic parameters have been kept the same as in Fig. 1 except ω_{12} is increased to 5 cm^{-1}. Since it is possible to find atoms with fine-structure splitting of the D states about 5 cm^{-1} and atomic parameters roughly of the same order of magnitude, we believe such an assumption is not unrealistic. On the other hand, this value of ω_{12} suffices to illustrate the effect under consideration.

Since $\omega_{12}=5$ cm^{-1}, $\delta=2\omega-\omega_{20}=0$, the $D_{3/2}$ state, being 5 cm^{-1} away from the $D_{5/2}$ state, influences the distribution even less compared to its influence in Fig. 1. Only at about 10^8 W/cm^2 does the distribution begin to lose its lobe structure due to the

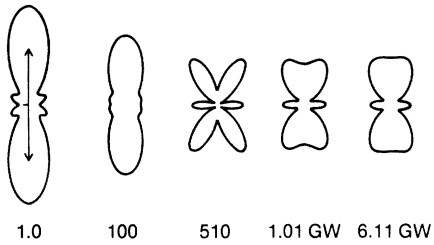

FIG. 3. Same as Fig. 1 except that the fine-structure splitting $\Delta=\omega_{4D_{3/2}}-\omega_{4D_{5/2}}=5\ \mathrm{cm}^{-1}$.

interference of the two channels. At these intensities, however, one is already in the saturation regime as $P\approx 1$ for $I\geq 5\times 10^8$ W/cm^2. Nevertheless, it is clear from this figure that the (limiting) distribution is still changing with increasing intensities. This is due to the fact that although $P=1$, it is not sufficient to infer that P_0,P_2,P_4, and P_6 have reached their limiting constant values. The evolution of $\rho_{11},\rho_{22},\rho_{12}$ is still sensitive to the laser parameters even though there is total ionization. Such effects are absent from Fig. 1 since the two D levels remain close together in the case pertinent to Fig. 1 while they are still well separated in the present case.

For the slowly varying model of the laser intensity as a function of time described earlier, the limiting values of the AD parameters p_{2k} obtained by numerical integration of Eqs. (1) and (26) agree with those obtained by the Laplace-transform method. For a more realistic laser pulse, however, one would expect to see some quantitative differences between the results obtained by the two methods while the qualitative features between them should remain the same.

The effects of laser bandwidth and its line shape are demonstrated in the next two figures. The finite bandwidth is assumed to arise due to the fluctuations of the phase of the electric field that are governed by an Ornstein-Uhlenbeck process. This model has been used recently in several related contexts[13,14] and the line shape is characterized by two parameters b and β; the former being the half-width at half maximum of the spectrum which is Lorentzian near the center and falls off faster than Lorentzian for detunings larger than the latter parameter β. For $\beta\rightarrow\infty$ the line shape is a Lorentzian for all detunings. A rigorous treatment of this type of a line shape leads to an infinite set of coupled moment equations as has been demonstrated elsewhere.[23] For β much larger than all other parameters one can retain the effect of the non-Lorentzian nature of the line shape to first order and the corrections to first order are of the form given in Eq. (1). It is clear from the form of the bandwidth-dependent terms in Eq. (1) that the effect of the phase fluctuations of the laser is to add a term $4b$ to the decay rate of the off-diagonal matrix elements ρ_{10} and ρ_{20} for detunings $\Delta_1,\Delta_2\ll\beta$. On the other hand, for large detunings $(\Delta_1,\Delta_2\gg\beta)$, these bandwidth-dependent terms in Eq. (1) vanish indicating the fact that the line shape looks monochromatic far off resonance. This treatment removes the unphysical absorptions from the wings of the spectrum in an off-resonant excitation process.

Figure 4(a) illustrates the effect of increasing bandwidth (b) on the angular distributions for the case $\omega_{12}=0.0346\ \mathrm{cm}^{-1}$ and $\delta=0$ while Fig. 4(b) does the same for the case $\omega_{12}=5\ \mathrm{cm}^{-1}$ and $\delta=-2\ \mathrm{cm}^{-1}$. The line shape is Lorentzian $(\beta\rightarrow\infty)$. Note that the bandwidth values are different for the two figures. In 4(a) the normalized distribution changes little for $b\gtrsim\omega_{12}$ as the levels become indistinguishable under broadband excitation and the distribution is insensitive to all saturation effects as discussed in Sec. II. The lobe structure is somewhat smeared out due to the increasing contribution from the absorption of photons from the wings of the spectrum by the off-resonant $D_{3/2}$ state. This is also seen in Fig. 4(b) since the distribution approaches a limiting

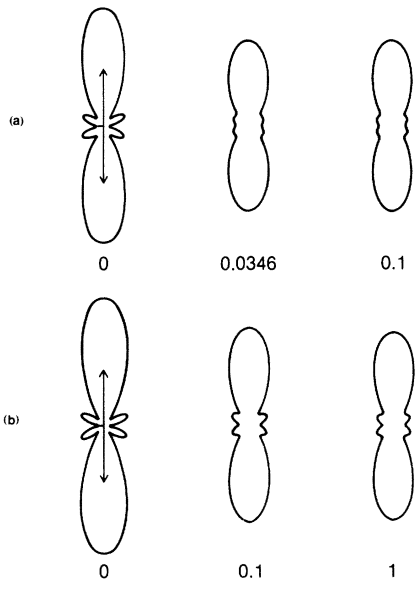

FIG. 4. Laser bandwidth effects on the angular distribution: (a) AD for $\Delta=0.0346\ \mathrm{cm}^{-1}$ and $\delta=0=(2\omega-\omega_{4D_{5/2}}+\omega_{3S_{1/2}})$; (b) AD for $\Delta=5\ \mathrm{cm}^{-1}$ and $\delta=-2\ \mathrm{cm}^{-1}$; $I=10$ MW/cm^2 and $T=5$ nsec for both sets of curves. The laser linewidth is assumed Lorentzian and the value for the half-width at half maximum (b in cm^{-1}) corresponding to each curve is indicated below it.

form even though $b < \omega_{12}, \delta$ for all the values. This distribution is similar to the one obtained by assuming only $D_{5/2}$ state participating in the process which is explained by the fact that the absorption from the wings by the $D_{5/2}$ state is stronger than that by the $D_{3/2}$ state since the latter is detuned farther (~ 7 cm^{-1}) from the center of the spectrum. This also explains the constancy of the distribution with respect to changes in the bandwidth.

The effects of the non-Lorentzian line shape (finite β) are demonstrated in Fig. 5 where the angular distributions are plotted for $\omega_{12}=5$ cm^{-1}, $\delta=0$, $\beta=100$, 0.2, 0.1 cm^{-1}, and $b=0.075$ cm^{-1}. Note that even for such small values of b (and $\beta=100$) the distribution is very different from the $b=0$ case in Fig. 3. As we decrease β the absorption of the photon from the tail of the spectrum by the off-resonant $D_{3/2}$ state decreases and hence the line shape looks more and more monochromatic thereby causing the distribution to revert to the $b=0$ result of Fig. 3.

IV. CONCLUSIONS

In summary, we have discussed the behavior of the photoelectron angular distributions in multiphoton ionization. A unified treatment of the strong-field effect on these distributions is developed in the density-matrix formalism. Saturation effects on the distributions appear in the form of coupling equations that involve the time-evolving density-matrix elements for the excited states. The theory of angular distributions is presented in a general form with completely general analytical expressions. On the basis of these, several conclusions have been arrived at and these are further illustrated with numerical results for two-photon resonant three-photon ionization of sodium. The effects of the laser line shape are also discussed.

The approximations of neglecting the spontaneous decay and the hyperfine structure in the results presented are valid for high laser powers and nsec pulses. Likewise, the pole approximation in eliminating the continuum is also valid as long as the continuum is smooth. Thus, except for the limitations introduced by the quantum-defect theory and the assumptions about the laser pulse shape, our results are rigorous and complete and are susceptible to direct experimental observation. With increasing experiments involving high-power lasers and resonant transitions, such complete calculations should prove to be useful in comparing experimental results with theoretical calculations and in extracting atomic parameters.

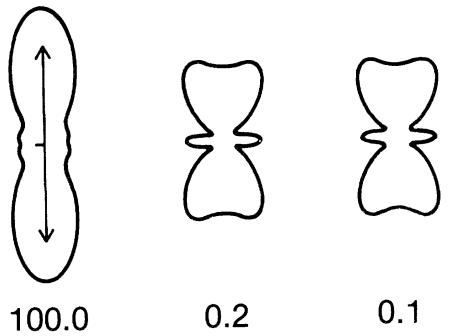

FIG. 5. Effects of the laser line shape on the photoelectron angular distributions: $\Delta=5$ cm^{-1}, $\delta=0$, $b=0.075$ cm^{-1}, $I=1$ GW/cm^2, and $T=5$ nsec. The cutoff parameter β is indicated, in cm^{-1}, below each curve. See text for details.

ACKNOWLEDGMENTS

The authors wish to thank Dr. G. Leuchs and Dr. H. Walther for several discussions. This work was supported in part by a grant from the National Science Foundation.

APPENDIX

In this appendix, we illustrate the procedure of adiabatic elimination of the continuum states leading to Eq. (8) for the angle resolved IP. Let H_0 and V denote, respectively, the unperturbed atomic Hamiltonian and the perturbation due to its interaction with the radiation field. The evolution of the density matrix ρ is governed by ($h=1$)

$$\frac{d\rho}{dt}=i[H_0+V,\rho]\ . \tag{A1}$$

Restricting ourselves to states $|1\rangle$, $|2\rangle$, and $|f\rangle$ defined in Sec. II, equations for the matrix elements of ρ between these states can be written, within the rotating-wave approximation, as

$$\frac{d\rho_{jj}}{dt}=2\,\mathrm{Im}\sum_f \rho_{jf}V_{fj},\quad j=1,2 \tag{A2}$$

$$\frac{d\rho_{ff}}{dt}=-2\,\mathrm{Im}(V_{f1}\rho_{1f}+V_{f2}\rho_{2f})\ ; \tag{A3}$$

$$\frac{d}{dt}\rho_{12}-i(\omega_1-\omega_2)\rho_{12}=i\rho_{1f}V_{f2}-iV_{1f}\rho_{f2}\ ; \tag{A4}$$

$$\frac{d\rho_{jf}}{dt}-i(\omega_j-\omega_f+\omega)\rho_{jf} = -iV_{jf}(\rho_{jj}-\rho_{ff})-i(\rho_{j2}V_{2f}\delta_{j1}+\rho_{j1}V_{1f}\delta_{j2})\ , \quad j=1,2\ . \tag{A5}$$

(Here δ_{ij} is the Kronecker δ function.) Note that the terms representing transition to the ground state are omitted from (A2) and (A4) for the sake of clarity. They are same as those given in Eq. (1).

We eliminate ρ_{jf},ρ_{fj} from (A2)–(A4) using the solution of (A5) obtained by setting $\rho_{ff}=0$ and $d\rho_{jf}/dt=0$ in (A5). This approximation amounts to treating the continuum as a sink for the loss of bound-state population and introduces the irreversibility of the flow of population into the continuum. Because of the large density of states in the continuum this approximation is adequate. The solution of (A5) under these approximations is given by

$$\rho_{jf}=\frac{iV_{jf}}{i(\omega_j+\omega-\omega_f)-\epsilon}\rho_{jj}+\frac{iV_{kf}}{i(\omega_j+\omega-\omega_f)-\epsilon}\rho_{jk}\ . \tag{A6}$$

$\rho_{fj}=\rho_{jf}^*$ and ϵ is real and positive and $\lim_{\epsilon\to 0}$ is taken in the end. Substituting (A6) into (A2)–(A4) one obtains

$$\frac{d}{dt}\rho_{jj}=2\,\mathrm{Im}\sum_f\left[\frac{|V_{jf}|^2}{\omega_j+\omega-\omega_f+i\epsilon}\rho_{jj}+\frac{V_{2f}V_{fj}\delta_{j1}}{\omega_j+\omega-\omega_f+i\epsilon}\rho_{j2}+\frac{V_{1f}V_{fj}\delta_{j2}}{\omega_j+\omega-\omega_f+i\epsilon}\rho_{j1}\right],\quad j=1,2 \tag{A7}$$

$$\frac{d}{dt}\rho_{12}-i(\omega_1-\omega_2)\rho_{12}=i\sum_f\frac{V_{1f}V_{f2}}{\omega_1+\omega-\omega_f+i\epsilon}\rho_{11}+i\sum_f\frac{|V_{2f}|^2}{\omega_1+\omega-\omega_f+i\epsilon}\rho_{12}$$
$$-i\sum_f\frac{V_{1f}V_{f2}}{\omega_2+\omega-\omega_f-i\epsilon}\rho_{22}-i\sum_f\frac{|V_{1f}|^2}{\omega_2+\omega-\omega_f-i\epsilon}\rho_{12}\ , \tag{A8}$$

$$\frac{d}{dt}\rho_{ff}=-2\,\mathrm{Im}\left[\sum_{j=1,2}\left[\frac{|V_{fj}|^2}{\omega_j+\omega-\omega_f+i\epsilon}\rho_{jj}\right]+\frac{V_{f2}V_{1f}}{\omega_1+\omega-\omega_f+i\epsilon}\rho_{12}+\frac{V_{f2}V_{1f}}{\omega_2+\omega-\omega_f+i\epsilon}\rho_{21}\right]. \tag{A9}$$

Note that the summation over f stands for integrations over the electron energy and its direction of propagation as well as a summation over its spin. Making use of the relation

$$\lim_{\epsilon\to 0}\frac{1}{x\pm i\epsilon}=\mathscr{P}\left[\frac{1}{x}\right]\mp i\pi\delta(x)\ ,$$

and assuming that the density of states in continuum is a slowly varying function of the energy, it is easy to see that (A7) and (A8) simplify to the terms given in Eq. (1), with

$$S_j-i\frac{\Gamma_j}{2}=\sum_f\frac{|V_{jf}|^2}{\omega_j+\omega-\omega_f+i\epsilon}\ ,\quad j=1,2$$

and

$$\Omega_{12}=2\sum_f\frac{V_{1f}V_{f2}}{\omega_1+\omega-\omega_f+i\epsilon}$$
$$\approx 2\sum_f\frac{V_{1f}V_{f2}}{\omega_2+\omega-\omega_f+i\epsilon}=\Omega'_{12}-i\Omega''_{12}\ .$$

Equation (A9) describes the details of the population distribution in the continuum. If energy analysis of the photoelectrons is not performed, we can integrate (A9) over the energy and define $P^{\pm}(\theta,\phi)$ as the total probability that electron will be ejected in a direction θ,ϕ and have spin $\pm\frac{1}{2}$. Correspondingly, one has to define angle- and spin-resolved width parameters $\Gamma^{\pm}_{1,2}(\theta,\phi)$ and $\Omega''^{\pm}_{12}(\theta,\phi)$ as

$$\Gamma^{\pm}_j(\theta,\phi)=2\pi\,|V_{jf}|^2\rho(k_f)\ ,\quad j=1,2$$
$$\Omega''^{\pm}_{12}(\rho,\phi)=2\pi V_{1f}V_{f2}\rho_f(\omega_f=\omega_1+\omega)\ , \tag{A10}$$

where

$$\tfrac{1}{2}k_f^2=\omega_1+\omega\ .$$

Final state $|f\rangle$ used in calculating matrix elements of V and the density of final states $\rho(k)$ are as defined in Eqs. (6) and (7). With (A10), (A9) immediately yields Eq. (8) of Sec. II.

[1]For a review of various aspects of multiphoton ionization processes, see, for example, the review by P. Lambropoulos, in *Advances in Atomic and Molecular Physics* (Academic, New York, 1976), Vol. 12, pp. 87–164.

[2]See *Multiphoton Processes*, edited by J. H. Eberly and P. Lambropoulos (Wiley, New York, 1978).

[3]J. C. Tully, R. S. Berry, and B. J. Dalton, Phys. Rev. 176, 95 (1968).

[4]M. Lambropoulos and R. S. Berry, Phys. Rev. A 8, 855 (1973).

[5]J. C. Hansen, J. A. Duncanson, Jr., R.-L. Chien, and R. S. Berry, Phys. Rev. A 21, 222 (1980).

[6]H. Kaminski, J. Kessler, and R. J. Kollath, Phys. Rev. Lett. 45, 1161 (1980).

[7]G. Leuchs, S. J. Smith, and H. Walther, in *Laser Spectroscopy IV,* edited by H. Walther and K. W. Rothe (Springer, Berlin, 1979), p. 225.

[8]A. T. Georges and P. Lambropoulos, in *Advances in Electronics and Electron Physics, Vol. 54* (Academic, New York, 1980), pp. 191–240.

[9]A preliminary account of this work has been published in S. N. Dixit and P. Lambropoulos, Phys. Rev. Lett. 46, 1278 (1981).

[10]B. L. Beers and L. Armstrong, Jr., Phys. Rev. A 12, 2447 (1975).

[11]S. N. Dixit and P. Lambropoulos, Phys. Rev. 21, 168 (1980).

[12]S. N. Dixit, P. Lambropoulos, and P. Zoller, Phys. Rev. 24, 318 (1981).

[13]P. Zoller and P. Lambropoulos, J. Phys. B 12, L547 (1979).

[14]I. Sobel'man *Introduction to the Theory of Atomic Spectra* (Pergamon, New York, 1972).

[15]A. Declémy, A. Rachman, M. Jaouen, and G. Laplanche, Phys. Rev. A 23, 1823 (1981).

[16]Note that this asymptotic form differs from that used in the tables by G. Peach [Mem. R. Astron. Soc. 71, 13 (1967)]. The asymptotic form of the radial wave function used by Peach is

$$\frac{1}{\sqrt{k}}\frac{1}{r}\sin\left[kr-\frac{l\pi}{2}-\delta_l\right].$$

Equations (3) and (4) would have different numerical factors in using Peach's wave function.

[17]M. Rotenberg, R. Bivins, N. Metropolis, and J. K. Wooten, Jr., *The 3-j and 6-j Symbols* (The Technology Press, Cambridge, Massachusetts, 1959).

[18]Y. Gontier, N. K. Rahman, and M. Trahin, J. Phys. B 8, L179 (1975).

[19]M. R. Teague and P. Lambropoulos, J. Phys. B 9, 1251 (1976).

[20]C. N. Yang, Phys. Rev. 74, 764 (1948).

[21]G. Nienhuis, E. H. A. Granneman, and M. J. Van der Wiel, J. Phys. B 11, 1203 (1978).

[22]C. E. Theodosiou, L. Armstrong, M. Crance, and S. Feneuille, Phys. Rev. A 19, 766 (1979).

[23]S. N. Dixit, P. Zoller, and P. Lambropoulos, Phys. Rev. A 21, 1289 (1980).